BODY FREEDOM FLUTTER OF A FLEXIBLE BLENDED WING BODY LIKE PLATE - AN EXPERIMENTAL STUDY

Yingsong Gu[1], Zhichun Yang[1], Pier Marzocca[2] and Shun He[1]

[1] Institute of Structural Dynamics and Control
Northwestern Polytechnical University, Xi'an 710072, China
guyingsong@nwpu.edu.cn, yangzc@nwpu.edu.cn, nwpuheshun@gmail.com

[2] School of Engineering (Aerospace Engineering and Aviation)
RMIT University, Bundoora, Victoria, 3083, Australia
pier.marzocca@rmit.edu.au

Keywords: body freedom flutter, blended wing body, aeroelasticity, wind tunnel test

Abstract: Aeroelastic modeling, analysis, and wind tunnel flutter test was conducted to investigate the body freedom flutter problem of a blended wing body (BWB) like flexible plate. The plate is made by aluminum with constant thickness of 0.2mm which resembles the shape of a high aspect-ratio configuration. Two types of suspension, i.e. nylon cord (D = 0.23mm) and bungee cord (D = 0.8mm), were implemented to study the influence of support stiffness on the body freedom flutter characteristics of the BWB like plate model. A gyro, attached on the upper surface of the plate model, was employed as sensor and connected to the data acquisition Arduino board by a flexible electric wire for data acquisition. It is found that both suspension types and the flexibility of the gyro's electric wire contribute to the support stiffness. While with the current suspension setup neither the free-free pitching mode, due to the added pitching stiffness coming from the flexible wire, not the free-free plunging mode, due to the suspension stiffness, could be accomplished, the flutter results predicted by an updated model accounting for the support stiffness, could produce quite satisfactory agreement with the test results. Lesson learned suggests that neither elastic nor rigid suspension can fully satisfy the body freedom flutter test requirement, and free-flying model setup is recommended for future wind tunnel test.

1 INTRODUCTION

As an unconventional configuration, *flying wing* is prone to an aeroelastic instability known as *Body Freedom Flutter* (BFF). BFF is a result of undesired dynamic coupling between the short period mode and the elastic wing bending mode [1, 2]. Previous works of the authors include numerical studies for the BFF characteristics of an open-loop high aspect ratio flying wing model [3] and also a closed-loop BWB flying wing model augmented with a flight control system [4].

Recently, Lockheed Martin developed the scaled BFF flying-wing aircraft, a 12-pound unmanned research vehicle with a 10 ft wingspan. Schmidt [5,6] and his coauthors [7,8] built the aeroelastic equations of motion (EOM) for this vehicle from first principle by coupling the flight-dynamics model and the aeroelastic model using vehicle-fixed, reference frame, and then developed an integrated control laws for stability augmentation and its active flutter suppression. Theis et al. [9] developed a robust control law base on H_∞ closed-loop shaping

for the same vehicle. System identification in flight was also conducted for this vehicle, using spectral analysis to identify the lightly damped structural modes and prediction error methods for estimating the aerodynamic parameters [10]. Ouellette [11] developed the aeroservoelastic model of the BFF research vehicle X-56A MUTT based on transformation of the structural and unsteady aerodynamic model from the inertial modal coordinate system into the non-inertial stability axis system. Huang et al. [12] studied the BFF boundary prediction of a half model for a BWB flying wing and interestingly found that the BFF instability is dominated by the coupling between the pitch mode and the second symmetric wing bending mode.

The study of the BFF instability is critical in the aeroelastic design of high aspect ratio flying wing, such as the BWB configurations, because of the rather low fundamental bending frequency of the wing. From a BFF test consideration point of view, flight flutter test has higher risk and is more expensive than the wind tunnel flutter test counterpart. However, the suspension system of the flutter model inside the wind tunnel is of particular concern, because the elastic support can alter the free-free pitching and/or plunging mode, leading to potential error in the flutter test result. For conventional configuration, this would not be a serious issue. However, for the BFF test, it may introduce significant discrepancy between test result and analytical result.

In the present work, a high aspect ratio BWB like plate model is designed, and a Nastran FEM and aeroelastic model is built to compute the normal modes and the flutter speed [13]. Additionally, a vibration and wind tunnel flutter test is conducted to investigate the model's dynamic and flutter characteristics, followed by model updating and the reexamination of the flutter speed with identified support stiffness of plunging and pitching degree of freedom of the plate. The plate is suspended mainly by the nylon cord or bungee cord on the vertical direction, assisted by other loose strings connected to the lower surfaces in case of large rigid body motion of the plate inside the wind tunnel. Two types of suspension strings, a nylon cord (with a diameter of D = 0.23mm) and a bungee cord (with a diameter of D=0.8mm), were implemented to study the influence of support stiffness on the body freedom flutter characteristics.

2 AEROELASTIC MODELING AND ANALYSIS OF FREE-FREE BWB PLATE

2.1 Model Geometric Description

The baseline of the current high aspect ratio BWB flying wing model is taken from [2] and is geometrically scaled down by 1/20 according to the test chamber size and the available speed of the wind tunnel, leading to a BWB like aluminum plate with constant thickness of 0.2mm as shown in Figure 1.

2.2 FEM and Aerodynamic Panel Modeling

The right half finite element model and aerodynamic panel model is built as shown in Figure 2. Symmetric boundary conditions are applied to the grid points along the symmetric line of the full model, only allowing the symmetric modes, such as free-free plunging/pitching, wing bending, and so on.

Shell elements are used to model the stiffness of the BWB model, while discrete mass elements are employed in this FEM to account for the inertial property of the balance weight and gyro sensor.

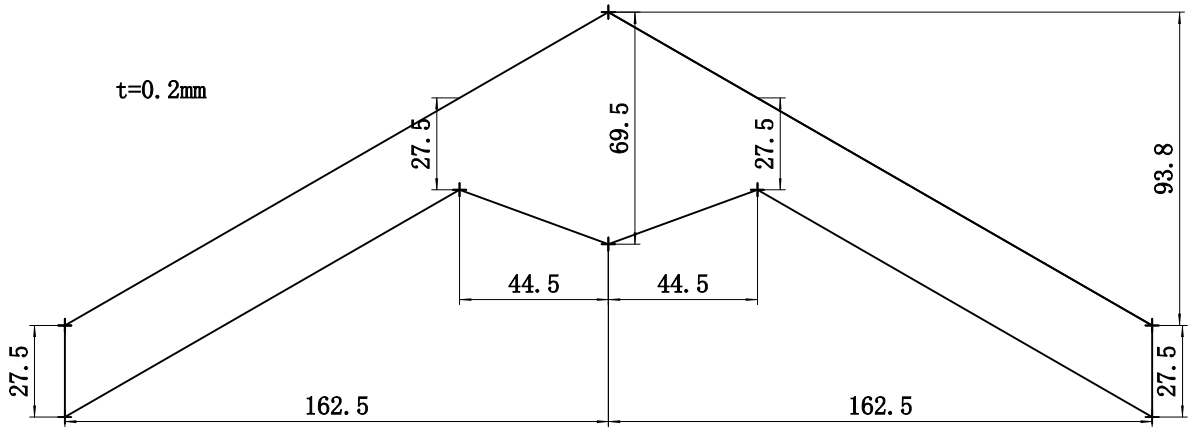

Figure 1: Schematic and dimensions of the BWB like plate in mm.

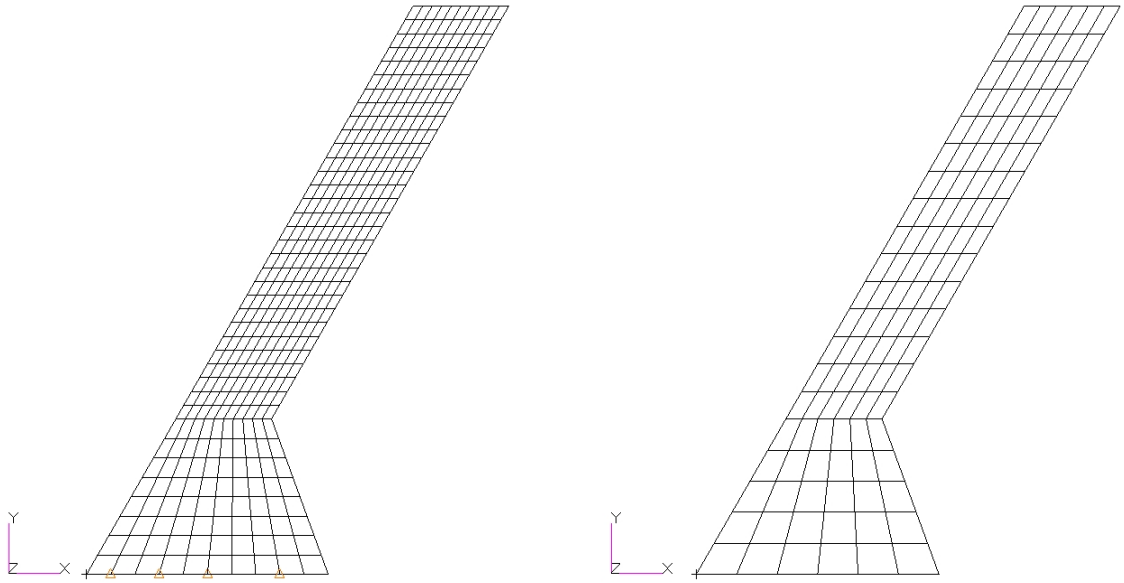

(a) (b)

Figure 2: FEM model (a) and panel aerodynamics model (b).

2.3 Normal Mode Analysis

Using the earlier described FE model, the normal modes are computed by MSC Nastran®. Only the symmetric modes of the right half model are obtained due to the symmetric boundary conditions. The free-free plunge/pitch mode and wing-1st symmetric bending mode are shown in Table 1 and Figure 3.

Mode	Description	*f*, Hz
1	plunge	0.0
2	pitch	0.0
3	wing 1st symmetric bending	6.91

Table 1: Free-free symmetric modes.

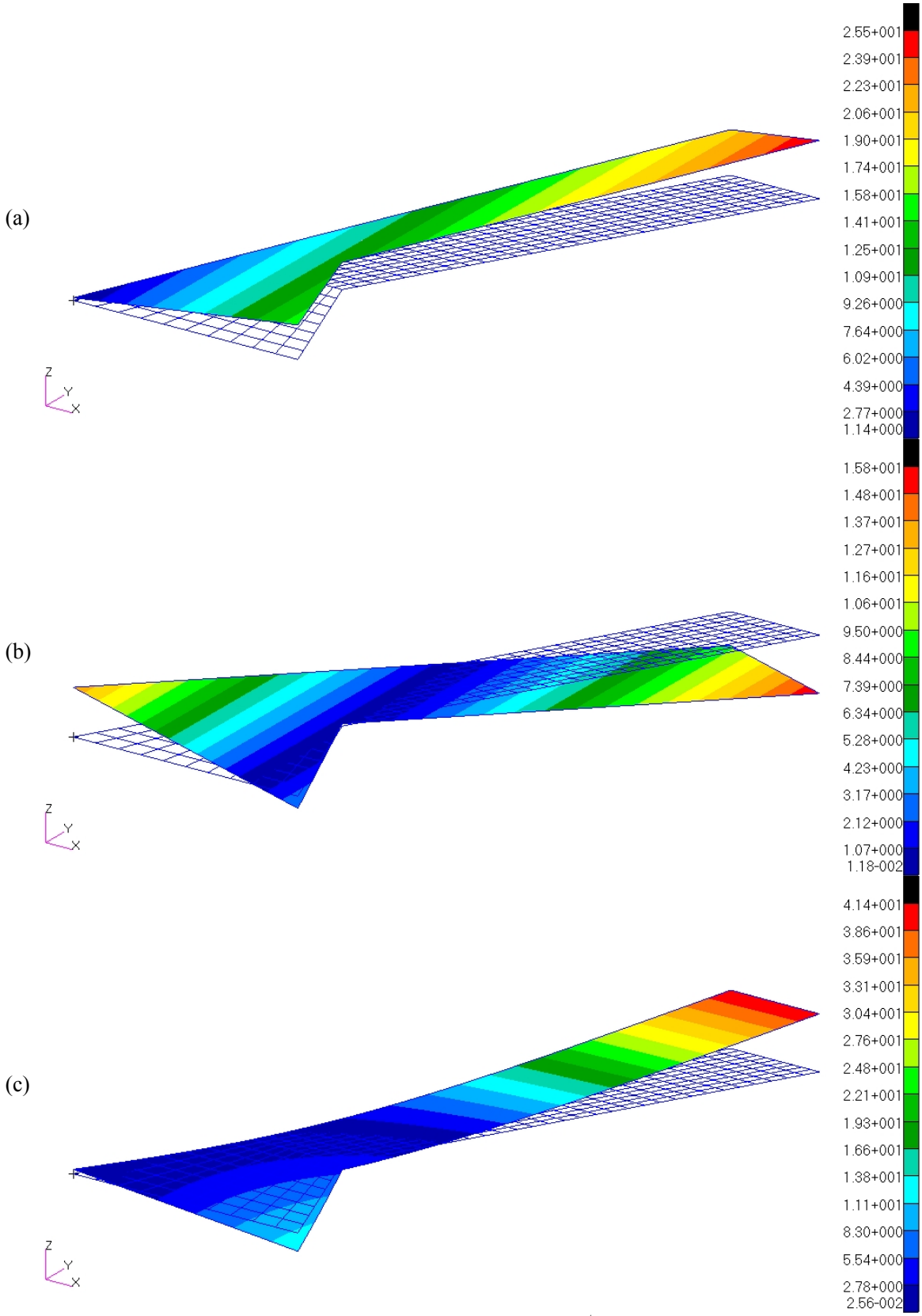

Figure 3: Free-free plunge mode (a), pitch mode (b) and wing-1st symmetric bending mode (c).

2.4 Body Freedom Flutter Analysis

In the flutter analysis, incompressible DLM aerodynamic model is utilized and the Infinite Panel Spline (IPS) method is employed to couple the structure model with the aerodynamic model. Considering the rigid body modes in addition to the elastic modes, body freedom flutter phenomenon is found for the present BWB plate model by the p-k method in Nastran. The V-g-f graph in Figure 4 shows a flutter speed of 5.9m/s, and flutter frequency of 5.27Hz for the free-free symmetric boundary conditions. There is very obvious frequency coalesce trend between the pitch mode (B labeled curve) and the wing 1st bending mode (C labeled curve), which is a typical characteristic in the body freedom flutter. Higher elastic branches are not shown in this figure due to lack of coupling.

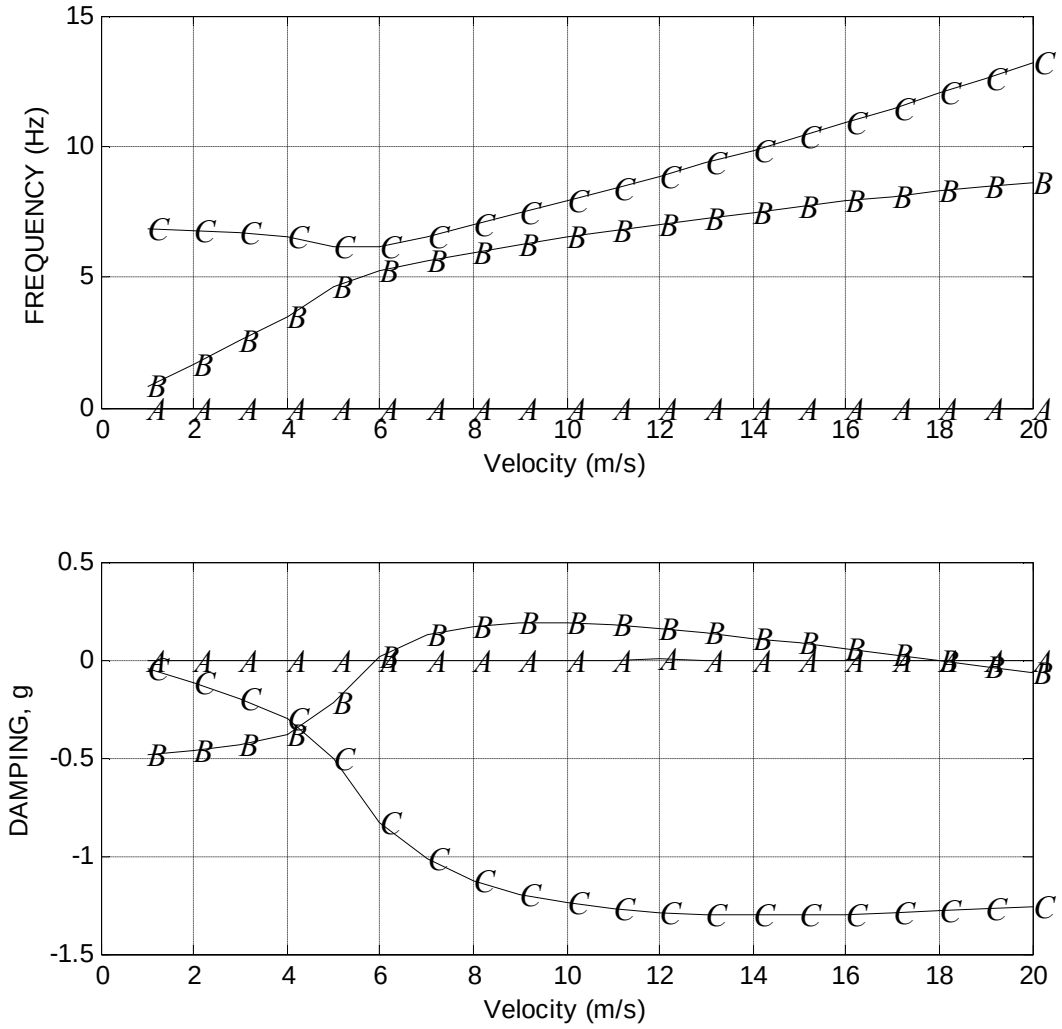

Figure 4: V-g-f graph of the theoretical model, A-plunge mode, B-pitch mode, C-wing 1st symmetric bending.

3 VIBRATION TEST AND MODEL UPDATING

3.1 Experimental Setup

The experiments were performed in the wind tunnel facility of the Department of Aeronautical Structural Engineering at Northwestern Polytechnical University (NPU, Xi'an, China). The tunnel is an Eiffel-type low speed, open return wind tunnel and the maximum airspeed is about 19.0 m/s. The test chamber is 28 cm long with an effective cross section of 30 cm in diameter.

The experimental setup is shown in Figure 5. The plate wing is suspended mainly by the nylon cord or bungee cord on the vertical direction, assisted by another two loose strings connected to the lower surfaces in case of seldom occurring large lateral rigid body motion of the plate. The vertical suspension string is also connected to a fixed point in the wind tunnel by a longitudinal string to hold its fore-aft motion, because there is no propulsion to balance the drag force.

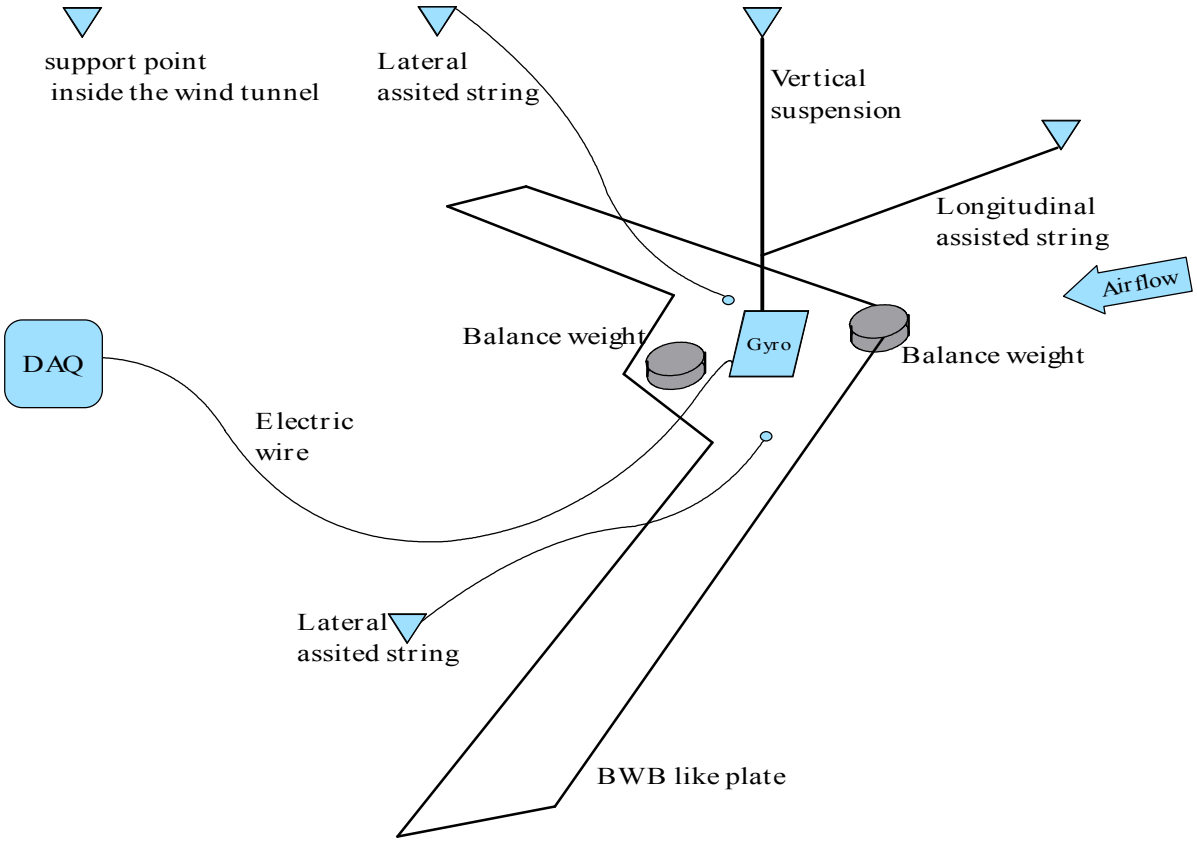

Figure 5: Test setup of the BWB like plate in the wind tunnel.

3.2 Sensor and Data Acquisition

Due to the scale of the current plate model, a MEMS sensor, MPU6050 Gyro is employed as the vibrometer, which can observe both the 6dof rigid body motion and the elastic motion of the test model. The location of the Gyro is near the mass center of test model. The data acquisition system as shown in Figure 6 is built by Arduino and Matlab with a sampling rate of 100Hz.

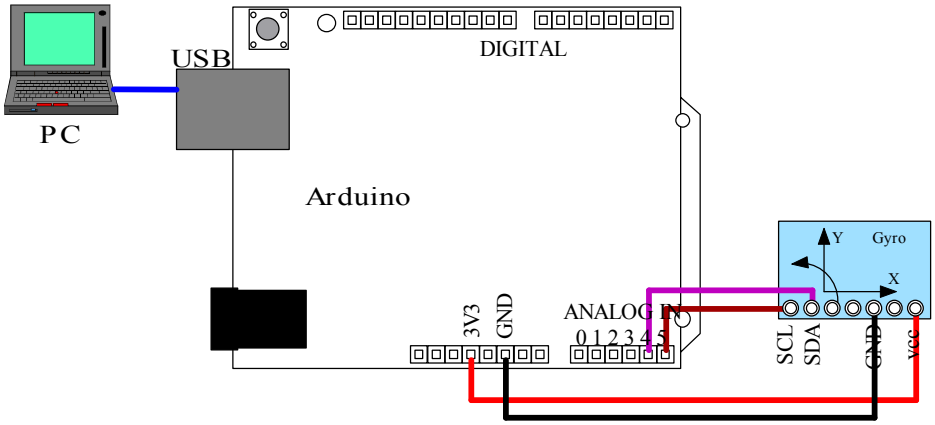

Figure 6: The data acquisition system.

3.3 Vibration Test Results

Two types of suspension string were applied, the nylon cord (D = 0.23mm) and bungee cord (D = 0.8mm). An impulse disturbance is applied to the suspended plate model, and the free response and frequency spectra of angular rates are recorded. Modal frequencies of dominant modes are identified and shown in Table 2. The plunge, pitch and wing 1st symmetric bending frequency can be identified from the spectra graph shown in Figure 7 for the bungee cord suspension case. However, for the nylon cord suspension, there is no plunge frequency found within the interested frequency range from the spectra graph shown in Figure 8. This can be explained by the fact that the nylon string is much stiffer than the bungee string. It should be mentioned that the nylon string can not resist compression load, thus it can be taken as a unilateral constraint.

In Figures 7 and 8, gx, gy, gz stands for fore-aft, side and vertical acceleration in the unit of g, respectively, and rx, ry, rz, stands for the roll, pitch and yaw angular rates in the unit of degree/s, respectively.

Due to the signal quality of the selected Gyro sensor, the angular rates are preferred in the frequency spectra analysis.

3.4 Model Updating

According to the test results, the pitch/plunge support stiffness is identified and introduced in the updated model, and the theoretical modal frequency is also shown in Table 2. It can be found the updated theoretical results are in quite good agreement with the test results. In the model updating procedure, the Young's modulus was also adjusted for this plate to match the wing 1st sym bending frequency.

Mode	Description	Nylon Cord			Bungee Cord		
		f_{exp}, Hz	f_{th}, Hz	Error,%	f_{exp}, Hz	f_{th}, Hz	Error,%
1	Plunge	N/A	N/A	N/A	4.04	3.99	-1.24
2	Pitch	3.38	3.24	-4.14	2.82	2.80	-0.71
3	wing 1st sym bending	7.98	7.71	-3.38	8.83	9.09	2.94

Table 2: Vibration test results in comparison with updated theoretical results.

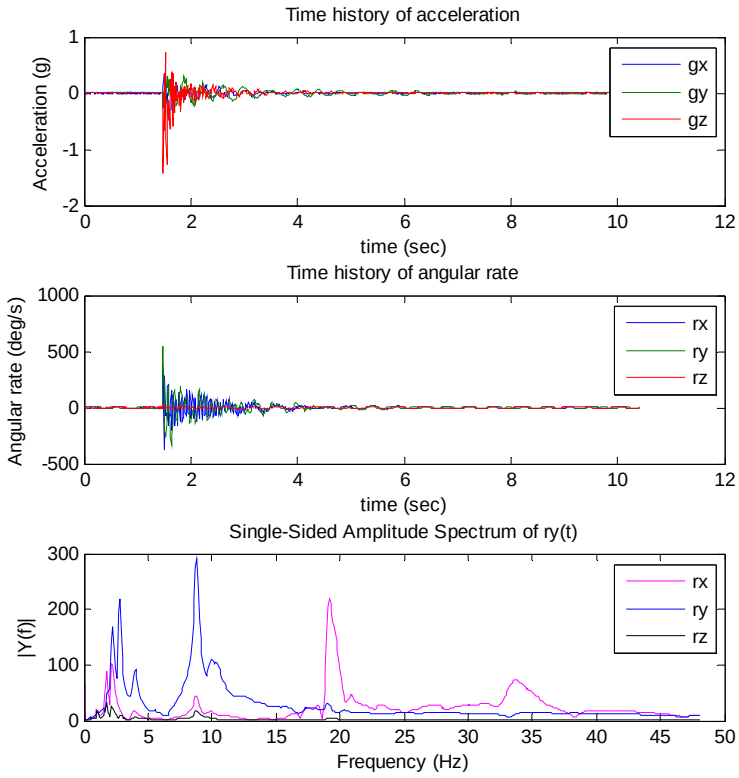

Figure 7: Time history and frequency spectra of free response, Bungee Cord suspension.

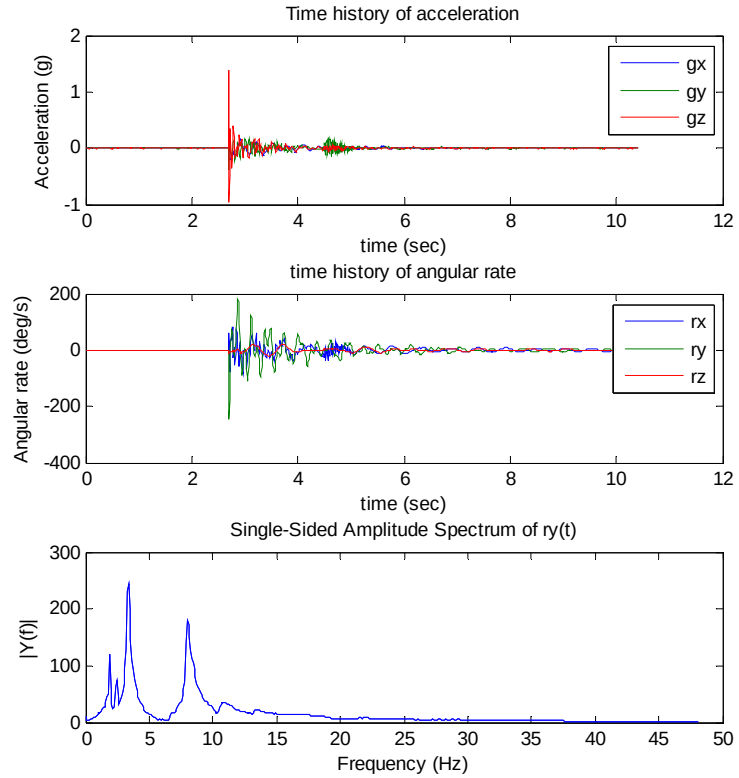

Figure 8: Time history and frequency spectra of free response, Nylon Cord suspension.

3.5 Reexamine the Flutter Characteristic

Using the updated FEM model, the flutter results are reexamined and shown in Table 3 for both suspension types. For the bungee cord suspension case, structure damping can increase the flutter speed over 15% by considering g = 0.03.

4 WIND TUNNEL FLUTTER TEST

Wind tunnel flutter test is conducted with the same sensor and data acquisition system as in the previous vibration test. The primary interests are the flutter onset condition and any post flutter behavior, such as limit cycle oscillations (LCOs).

4.1 Flutter Onset Test Results

During the test, free response is recorded for the model under an initial impulse disturbance at a given airspeed, and then the airspeed is increased slowly until a diverging vibration motion is detected. In addition, the aeroelastic response due to the inherent turbulence inside the wind tunnel is also recorded.

The flutter onset speed and frequency under nylon cord or bungee cord suspensions are shown in Table 3 in comparison with the updated theoretical results. It should be noted that we observe a range of airspeed of 3.2~3.7 m/s for the flutter onset under the bungee cord suspension. This may be attributed to the unstable wind tunnel flow condition for this relative low speed range.

Case	Suspension type	Flutter test results		Theoretical results g=0		Theoretical results g=0.03	
		V_F, m/s	f_F, Hz	V_F, m/s	f_F, Hz	V_F, m/s	f_F, Hz
1	Nylon Cord	5.2	5.8	4.4	4.9	4.6	5.0
2	Bungee Cord	3.2~3.7	3.5	2.7	3.10	3.15	3.3

Table 3: Flutter test results in comparison with updated theoretical results.

For the nylon cord suspension case, the flutter mode can be illustrated by snap shot sequence as shown in Figure 9. This was recorded in the experiment without sensor and data acquisition. Figure 9(a) depicts the equilibrium state under a very low airspeed before flutter point. Figure 9(b) and Figure 9(c) show the typical body freedom flutter mode just after the flutter onset, i.e. strong coupling between pitching and wing 1st symmetric bending mode.

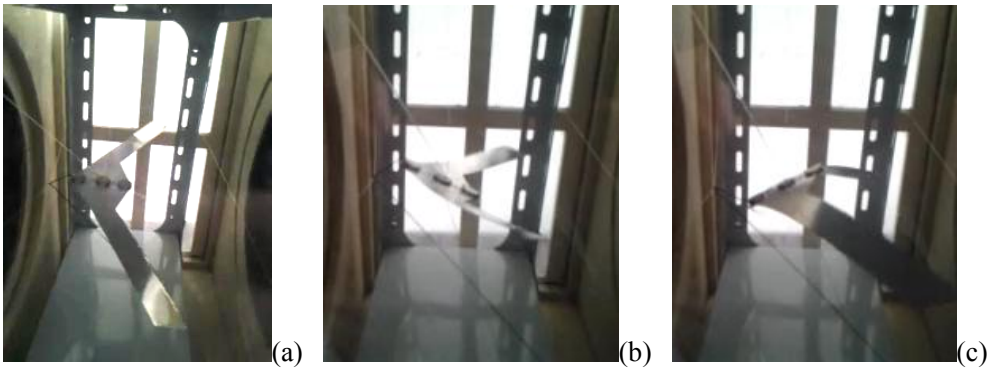
(a) (b) (c)

Figure 9: Snap shot for the BFF mode visualization, Nylon Cord suspension.

4.2 Sub Critical and Critical Response

Sub critical and critical response observed by the Gyro was recorded. For the Nylon Cord suspension case, the corresponding results are shown in Figures 10 and 11. For the Bungee Cord suspension case, the corresponding results are shown in Figures 12 and 13. As stated in Section 3.3, gx, gy, gz stands for fore-aft, side and vertical acceleration in the unit of g, respectively, and rx, ry, rz, stands for the roll, pitch and yaw angular rates in the unit of degree/s, respectively.

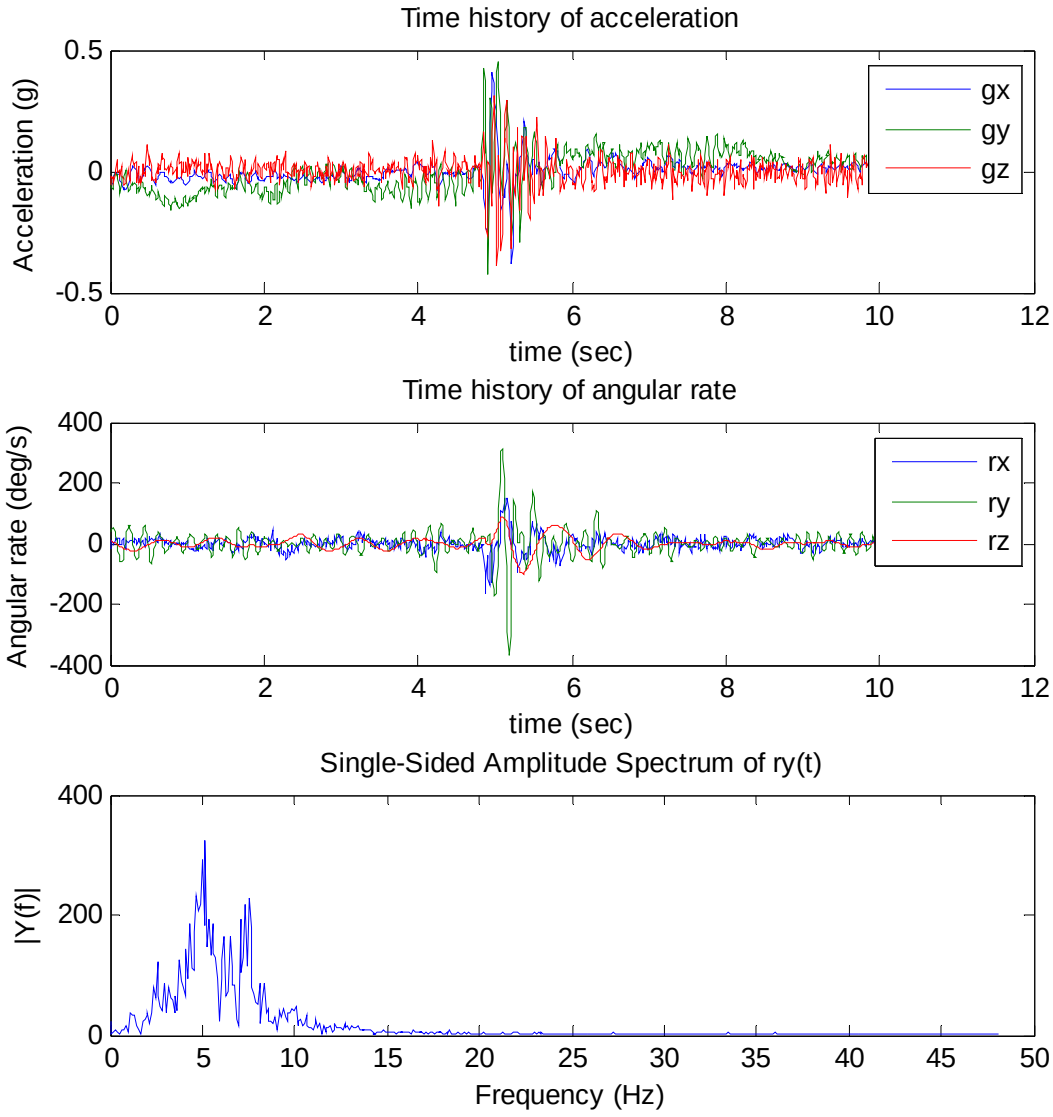

Figure 10: Sub critical response with pulse disturbance, Nylon Cord suspension, V=4.3 m/s.

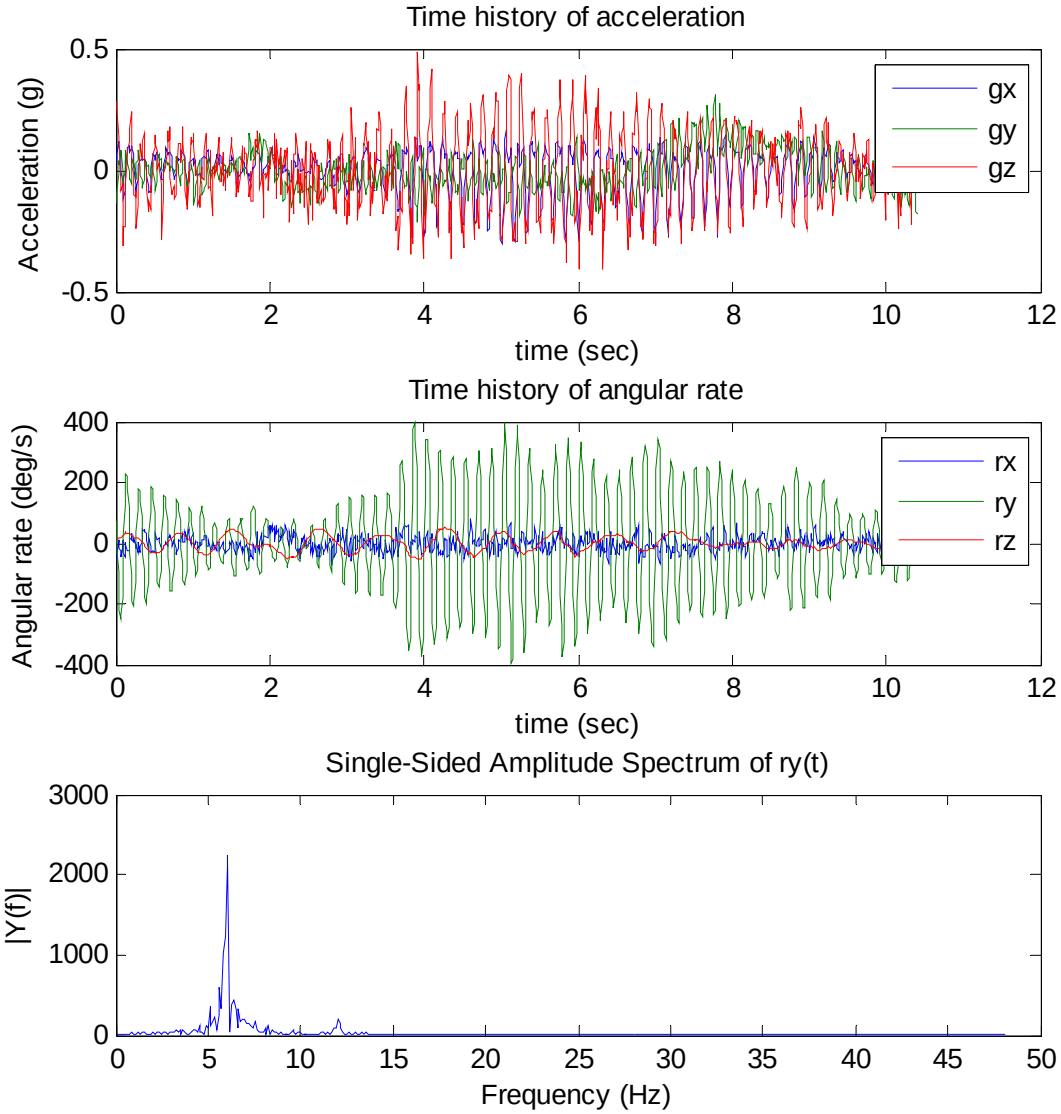

Figure 11: Critical response with turbulence disturbance, Nylon Cord suspension. V=5.2m/s

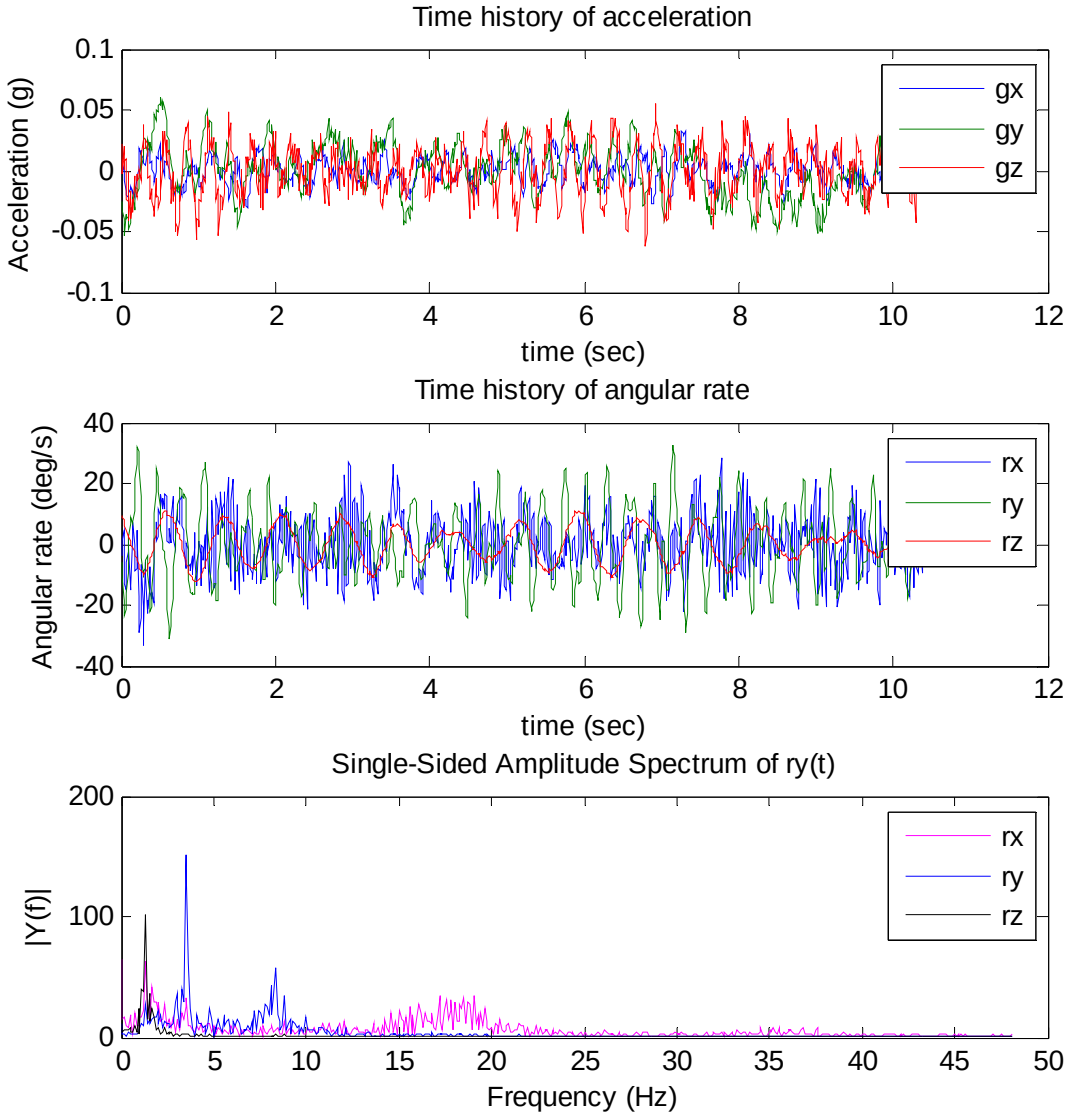

Figure 12: Sub critical response with turbulence disturbance, Bungee cord suspension. 3.2m/s

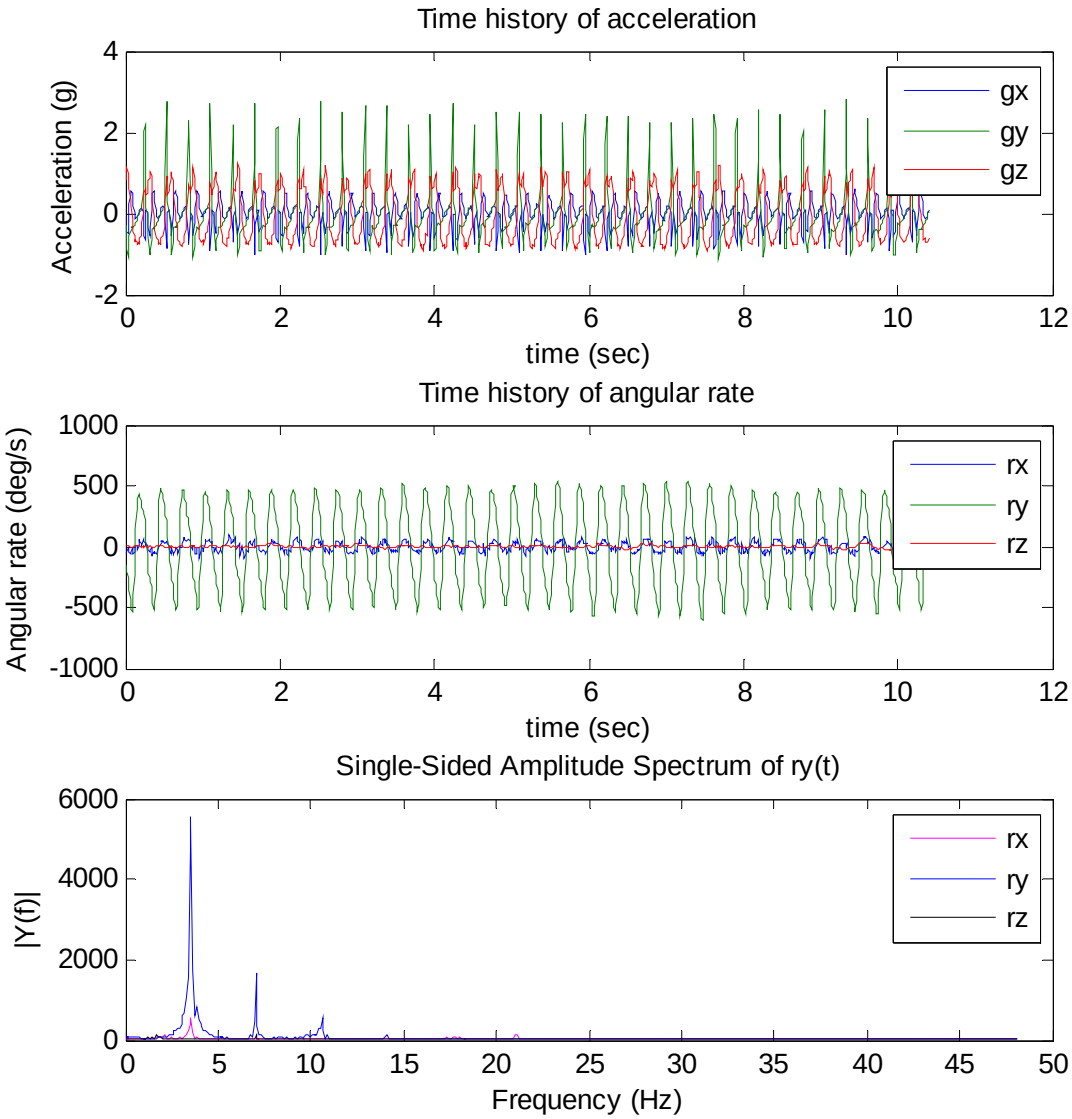

Figure 13: Critical response with turbulence disturbance, Bungee cord suspension. V=3.7m/s

4.3 Post Flutter Test and LCO

An LCO was also observed from the above critical flutter response. Large amplitude LCO is found in the post flutter test as the airspeed exceeds 5.3m/s for the nylon cord suspension case, and 3.7m/s for the bungee cord case. Interestingly, period doubling is clearly depicted in Figure 13, from which one can find that the vertical acceleration (gy) response is much larger in the positive (up) direction than in the negative one. It is implied that the nonlinear plunging stiffness in large amplitude motion may be a dominate factor leading to such a complex LCO.

The bifurcation graph for the pitch rate and pitch frequency versus airspeed is shown in Figures 14 and 15 for the nylon cord and bungee cord case, respectively. It is found the pitch rate develops quickly as the airspeed exceeds the critical flutter speed. Because the frequency only varies moderately, it can be inferred that the pitch amplitude will also increase quickly in the post flutter region.

The current flat plate model has no airfoil shape, so it is quite easy to enter stall region at moderate amplitude of angle of attack. Strong aerodynamic (dynamic) stall nonlinearity may be the dominated nonlinearity resource that restricts the developing of the large amplitude of LCO.

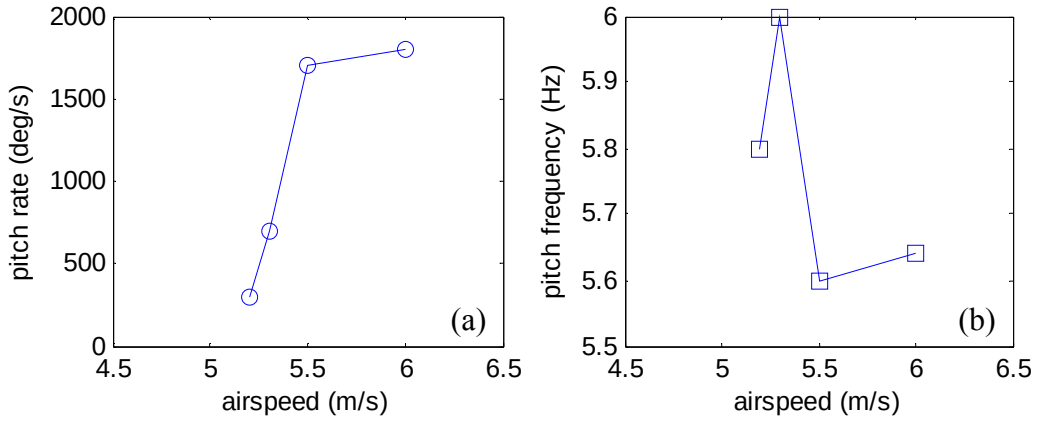

Figure 14: Bifurcation graph for the pitch rate (a) and pitch frequency (b) vs airspeed, Nylon Cord suspension.

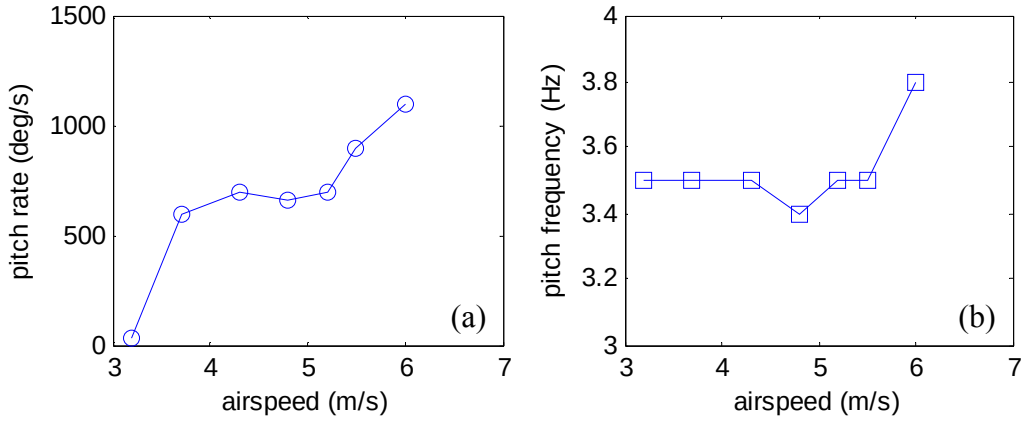

Figure 15: Bifurcation graph for the pitch rate (a) and pitch frequency (b) vs airspeed, Bungee Cord suspension.

5 DISCUSSIONS AND CONCLUDING REMARKS

In this work, a low cost body freedom flutter experiment is conducted using a small size Eiffel-type wind tunnel. It is demonstrated that with properly designed size parameters, BFF can occur for a BWB like plate at a very low airspeed of only several meters per second, which is well within the available operation range of this test facility.

The current test model setup cannot reproduce theoretically “free-free” pitching mode due to the added pitching stiffness of the flexible electric wire. The same setup cannot reproduce “free-free” plunging mode either due to the suspension stiffness in the wind tunnel. As a consequence, the flutter speed under elastic suspension can be quite different from the true free-free case.

Elastic or rigid suspension cannot fully satisfy the body freedom flutter test requirement, and a free-flying model is recommended to be implemented in wind tunnel tests. This was demonstrated in [14] albeit with a more complicated closed-loop test setup.

Despite the above limitations, theoretical modal and flutter results using the updated FEM model achieve a reasonably good agreement with the test results, giving confidence in the general understanding of the flutter behavior which has been reproduced in the wind tunnel.

6 ACKNOWLEDGEMENT

This research was financially supported by the National Natural Science Foundation of China (Grant Nos. 11102162，11672240 and 11072198). The first author wishes to thank Chengzhe Zou for technical assistance in the modal test.

7 REFERENCES

[1] Love, M. H., Zink, P. S., Wieselmann, P. A. and Youngren H. (2005). Body freedom flutter of high aspect ratio flying wings. AIAA-2005-1947.

[2] Su, W.H. and Cesnik, C.E.S. (2010). Nonlinear aeroelasticity of a very flexible blended-wing-body aircraft. *Journal of Aircraft*, 2010, 47(5):1539-1553.

[3] Li, Y.D., Zhang, X.P., Gu, Y.S. and Yang Z.C. (2014).Body freedom flutter study and passive flutter suppression for a high aspect ratio flying wing model. 4th International Conference on Intelligent Structure and Vibration Control, July 25-28, 2014, Chongqing, China.

[4] Gu Y.S., Yang Z.C. and He, S. (2014).Body freedom flutter of a blended wing body model coupled with flight control system. 2014 Asia-Pacific International Symposium on Aerospace Technology, APISAT2014, September 24-26, Shanghai, China.

[5] Schmidt, D. K. (2016). MATLAB-Based Flight-Dynamics and Flutter Modeling of a Flexible Flying-Wing Research Drone. *Journal of Aircraft*, 53(4), 1045-1055.

[6] Schmidt, D. K. (2016). Stability Augmentation and Active Flutter Suppression of a Flexible Flying-Wing Drone. *Journal of Guidance, Control, and Dynamics*, 39(3), 409-422.

[7] Schmidt, D. K., Zhao, W. and Kapania, R. K. (2016). Flight-Dynamics and Flutter Modeling and Analysis of a Flexible Flying-Wing Drone. AIAA-2016-1748.

[8] Keyes, S.A., Seiler, P, and Schmidt, D. K. (2017). A Newtonian Development of the Mean-Axis Equations of Motion for Flexible Aircraft. AIAA-2017-1395.

[9] Theis, J., Pfifer, H. and Seiler P. (2016). Robust Control Design for Active Flutter Suppression. AIAA-2016-1751.

[10] Pfifer, H. and Danowsky B. (2016). System Identification of a Small Flexible Aircraft. AIAA-2016-1750.

[11] Ouellette, J. (2017). Aeroservoelastic Modeling of Body Freedom Flutter for Control System Design. AIAA-2017-0019.

[12] Huang, C., Wu, Z.G., Yang, C. and Dai Y.T. (2017). Flutter Boundary Prediction for a Flying-Wing Model Exhibiting Body Freedom Flutter. AIAA-2017-0415.

[13] Rodden, W. P. and Johnson, E. H. (1994). *MSC/NASTRAN Aeroelastic Analysis User's Guide*, Ver. 68, MacNeal-Schwendler, Los Angeles, 1994.

[14] Scott, R. C., Vetter, T. K., Penning, K. B., Coulson, D. A. and Heeg, J. (2008). Aeroservoelastic Testing of a Sidewall Mounted Free Flying Wind-Tunnel Model. AIAA 2008-7186

COPYRIGHT STATEMENT